Electric Field in a Double Layer and the Imparted Momentum

A. Fruchtman

Holon Academic Institute of Technology, 52 Golomb Street, Holon 58102, Israel
(Received 27 September 2005; published 14 February 2006)

It is shown that the net momentum delivered by the large electric field inside a one-dimensional double layer is zero. This is demonstrated through an analysis of the momentum balance in the double layer at the boundary between the ionosphere and the aurora cavity. For the recently observed double layer in a current-free plasma expanding along a divergent magnetic field, an analysis of the evolution of the radially averaged variables shows that the increase of plasma thrust results from the magnetic-field pressure balancing the plasma pressure in the direction of acceleration, rather than from electrostatic pressure.

The strong electric fields confined to narrow isolated regions in plasmas, called double layers (DL) [1], have been suggested to accelerate particles in the aurora [2], cosmic rays [3], laser-ablated plasmas [4], laboratory experiments [5], and recently in gas discharges [6–9]. In this Letter we show that the net force and momentum imparted by these strong electric fields in a one-dimensional (1D) DL are identically zero. We demonstrate this often-overlooked vanishing of force and momentum by analyzing the DL located at the boundary between the ionosphere and the aurora cavity [10]. For the DL recently observed in the common configuration of an axially current-free plasma expanding along a divergent magnetic field [6–8], we show that the increase of plasma thrust results from the magnetic field pressure that balances the plasma pressure in the direction of acceleration, rather than from electrostatic pressure. This unfolding of the mechanism of DL acceleration is important for the development of accelerators and thrusters and for understanding many phenomena in space [11]. In general, an insight into momentum balance is important since evidence of a DL existence in distant astrophysical objects must rely on its global aspects [1,12].

The contribution of the electric field to the momentum is deduced from application of the divergence theorem to the momentum equations. If the electromagnetic pressure tensor elements are zero at the domain boundaries, the electromagnetic fields do not affect the total mechanical momentum. In a 1D DL this statement is exhibited very clearly. Multiplying the two sides of the equation that expresses Gauss law by the electric field, we obtain $\epsilon_0 \vec{\nabla} \cdot \vec{E} \vec{E} = \rho \vec{E}$, where $\vec{E}$ is the electric field, ρ the net charge density, and ϵ_0 the permittivity of free space. If all variables depend on z only, the integral form of this equation becomes

$$\frac{\epsilon_0}{2}[E(z_2)^2 - E(z_1)^2] = \int_{z_1}^{z_2} \rho E dz. \qquad (1)$$

The total electric force equals the difference between the electrostatic pressures on the two boundaries of the domain (z_1 and z_2). In a DL the electric field is zero at the two

boundaries. Thus, the total force exerted and the momentum delivered by the electric field of a 1D DL are zero.

As a concrete example we construct a collisionless-plasma DL configuration in which, for simplicity, the trapped (reflected) particle populations have water-bag distributions [13], while the free particle populations are two cold counter-propagating ion and electron beams. We assume the electric potential $\phi(z)$ at the two sides of the DL to be $\phi(z = -\infty) = 0$ and $\phi(z = \infty) = -\phi_0$ ($\phi_0 > 0$). Poisson's equation is written as

$$\frac{\epsilon_0}{e} \frac{d^2\phi}{dz^2} = -\frac{n_{\text{fi}}}{\sqrt{1 - e\phi/\varepsilon_{\text{fi}}}} + \frac{n_{\text{fe}}}{\sqrt{1 + e(\phi + \phi_0)/\varepsilon_{\text{fe}}}}$$
$$- n_{\text{ti}}\sqrt{1 - \frac{e(\phi + \phi_0)}{\varepsilon_{\text{ti}}}} + n_{\text{te}}\sqrt{1 + \frac{e\phi}{\varepsilon_{\text{te}}}}, \qquad (2)$$

where the first two terms on the right-hand side (RHS) of the equation represent the densities of the ion and electron beams, while the third and fourth terms represent the densities of the trapped ion and electron populations. The maximal densities of the four particle groups are n_{fi} (free ions), n_{fe} (free electrons), n_{ti} (trapped ions), and n_{te} (trapped electrons). The kinetic energies of the beam particles moving towards the DL are ε_{fi} (ions) and ε_{fe} (electrons) and the maximal energies of the trapped ions and electrons are ε_{ti} and ε_{te} (both are smaller than $e\phi_0$, e being the elementary charge). Upon integrating Eq. (2) from $z = -\infty$ we obtain an equation [which is Eq. (1) for this case] that expresses the momentum balance:

$$\frac{\epsilon_0}{2}\left(\frac{d\phi}{dz}\right)^2 = 2n_{\text{fi}}\varepsilon_{\text{fi}}\left(\sqrt{1 - \frac{e\phi}{\varepsilon_{\text{fi}}}} - 1\right)$$
$$+ 2n_{\text{fe}}\varepsilon_{\text{fe}}\left(\sqrt{1 + \frac{e(\phi + \phi_0)}{\varepsilon_{\text{fe}}}} - \sqrt{1 + \frac{e\phi_0}{\varepsilon_{\text{fe}}}}\right)$$
$$+ \frac{2n_{\text{ti}}\varepsilon_{\text{ti}}}{3}\left[1 - \frac{e(\phi + \phi_0)}{\varepsilon_{\text{ti}}}\right]^{3/2}$$
$$+ \frac{2n_{\text{te}}\varepsilon_{\text{te}}}{3}\left[\left(1 + \frac{e\phi}{\varepsilon_{\text{te}}}\right)^{3/2} - 1\right]. \qquad (3)$$

The first two terms on the RHS of the equation are the

momenta changes (with respect to the high potential side at $z = -\infty$) of the ion and of the electron beams. The third term and the fourth term are the pressure changes of the trapped ions and electrons, respectively. The third term on the RHS of both last equations is zero when $\phi \geq \varepsilon_{ti}/e - \phi_0$, while the fourth term is zero when $\phi \leq -\varepsilon_{te}/e$.

The various net contributions to the momentum are obtained by Eq. (3) at $z = \infty$, where the electric field is zero. The change in the total momenta of the beams equals the change in total pressure of the trapped particles. Although the electrostatic pressure does deliver momentum locally inside the DL, the total momentum it imparts across the DL is zero. Examples of the profiles of variables for a symmetrical DL (the electric-field intensity depends on the distance from the plane of symmetry at the center of the DL) and an asymmetrical DL are shown in Fig. 1. Charge neutrality, zero electric field, and appropriate Bohm conditions are imposed at the two boundaries for obtaining the DL solutions. For the asymmetrical DL the parameters were chosen to be similar to those at the DL between the ionosphere and the aurora cavity. Such is the ratio of 10 between the plasma densities on the two sides of the DL [10]. The various contributions to the momentum balance, shown in Figs. 1(d) and 1(h), exhibit the local nonzero contribution of the electrostatic pressure and the global vanishing of that contribution. It is interesting to note that despite the fact that the density of the precipitating electrons, presented here as the cold beam, is low, their change of momentum is large. In fact, as is shown in Figs. 1(d) and 1(h), it is that momentum change of the precipitating electrons that balances the opposite momentum change of the high-density ion beam.

When electromagnetic energy is converted into particle energy in the DL, a source of energy, a battery, has to exist outside the DL. On the other hand, if the particle motion is reversed, so that particle energy becomes electromagnetic energy, the DL itself acts as a battery. Thus, the electric field in the DL does exchange energy with, but does not impart momentum to the particles.

The above demonstrated vanishing of the force on the plasma in a 1D DL does not necessarily occur in DLs in a plasma flow of a varying cross section for which Eq. (1) is not valid. For the analysis we employ a standard quasi-1D model of the flow along streamlines, in which all radially averaged variables vary along z only, as does the cross section of the flow $A(z)$ [14]. The governing equations are $(1/A)d(mn_i v^2 A)/dz = -en_i d\phi/dz - F$ and $0 = en_e d\phi/dz - d(n_e T)/dz$, where n_i and n_e are the ion and electron densities, v, m, and F the ion velocity, mass and drag force. The electron temperature is T, while the ions are assumed cold. In the isothermal case we treat here the electron density and the electric potential obey the familiar Boltzmann relation. Summing the governing equations and employing Poisson's equation, we obtain the general momentum balance equation:
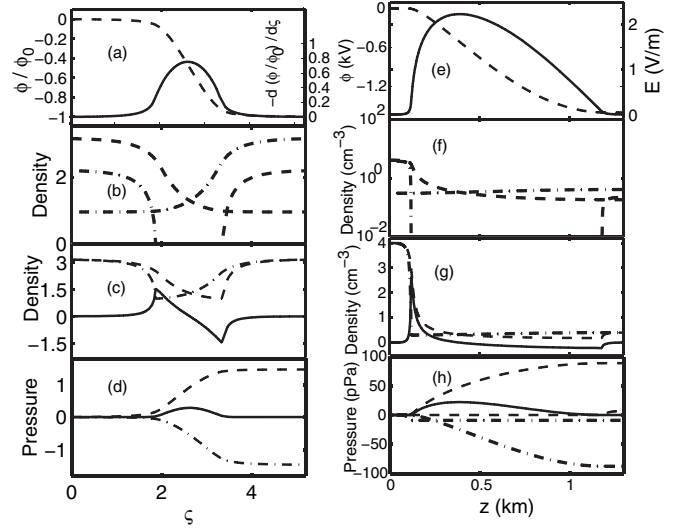

FIG. 1.   Left: a symmetrical double layer (dimensionless quantities)—the electric field (solid line) is $d(\phi/\phi_0)/d\varsigma$, the potential (dashed line) ϕ/ϕ_0, densities normalized to $n_{fi}\sqrt{\varepsilon_{fi}/e\phi_0}$, pressures to $n_{fi}\sqrt{e\phi_0\varepsilon_{fi}}$, and $\varsigma \equiv z/[(\epsilon_0/n_{fi})^{1/2}\phi_0^{3/4}/(e\varepsilon_{fi})^{1/4}]$. Right: an asymmetrical double layer (similar to that at the ionosphere—aurora cavity DL). (a),(e) The potential and the electric field, (b),(f) the densities of the four populations, (c),(g) the total ion and electron densities and the difference between them, (d),(h) the pressure terms on the RHS of Eq. (3) for the four populations and the electrostatic pressure. Ion variables are shown as dashed lines, electron as dash-dotted lines; the difference between ion and electron densities in (c),(g) and the electrostatic pressure in (d),(h), as solid lines. The pressure of the trapped particles in the symmetrical case is too small to be shown.

$$\frac{d}{dz}\left[mn_i v^2 A + n_e TA - \frac{\epsilon_0}{2}\left(\frac{d\phi}{dz}\right)^2 A\right] + FA$$
$$= \left[n_e T - \frac{\epsilon_0}{2}\left(\frac{d\phi}{dz}\right)^2\right]\frac{dA}{dz}. \quad (4)$$

The electric field is zero on both sides of the DL in the z direction along the flow and therefore has no net contribution to the momentum through the 1D momentum balance, expressed by the left-hand side of the equation. The electric field however, does impart a net momentum according to the RHS of the equation (due to a contribution to the electric field from charges that are outside the flow). That RHS of the equation expresses the z component of the flux of the total pressure tensor across the radial boundaries, a component that is not zero when the cross section varies. Both the mechanical pressure flux and the electrostatic pressure flux through the radial boundaries do impart net momentum. However, that momentum delivered by the electrostatic pressure is small, even locally, when acceleration occurs in the quasineutral regime. Assuming quasineutrality, $n \equiv n_i = n_e$, we write the equation for the Mach number $M \equiv v/c$, where $c \equiv \sqrt{T/m}$ is the isothermal sound speed, in a form that exhibits the sonic critical point:

$$(M^2 - 1)\frac{dM}{dz} = M\frac{d\ln A}{dz} - (M^2 + 1)\frac{\nu}{c} - \frac{F}{nmc^2}. \quad (5)$$

We used the continuity equation, $d(n\nu A)/dz = \nu nA$, ν being the ionization frequency. The acceleration to supersonic velocities requires that the RHS of the equation change sign at the sonic plane [15]. We note in passing that Eq. (5) also describes the acceleration of the solar wind to supersonic velocities [16], in which the drag force is sun gravity, $F = GM_\Theta mn/z^2$ (G is the gravitation constant, M_Θ the mass of the sun, and z the distance from the center of the sun), A/z^2 is constant and $\nu = 0$. The isothermal acceleration is described by one of the solutions for M of the following (Bernoulli) equation: $M^2 - \ln M^2 = 4(\ln z/z_s + z_s/z) - 3$, the characteristic length is on the order of $z_s \equiv GM_\Theta/2c^2$, at which the sonic transition occurs. For $T = 500$ eV z_s equals twice the sun radius, so that the acceleration is *not* localized but rather occurs across a large part of the corona.

It has been proposed that plasma acceleration should occur when the increasing cross section of the flow results from a strong divergent magnetic field, so that $B(z)A(z) = $ const, $B(z)$ being the intensity of the magnetic field [17]. The external force that balances the plasma pressure at the radial boundaries is the magnetic-field force, and its z component, expressed by the RHS of Eq. (4), increases the plasma thrust Th $\equiv mn\nu^2A + nTA$ along the flow. This axial magnetic-field force equals the product of an azimuthal plasma current and the radial component of the varying magnetic field, as could be exhibited by a 2D model that describes both radial and axial variations, such as that in Ref. [18]. Localized acceleration to supersonic velocities can occur when $\nu = F = 0$ if the magnetic-field lines first converge and then diverge along the flow as in the Laval nozzle. With a nozzle configuration, such as $A = A_s\{1 + \ln[1 + (z/L)^2]\}$, the relations between the flow variables, $A = (A_s/M)\exp[(M^2 - 1)/2]$, $n = n_s\exp[(1 - M^2)/2]$, and $\phi_N \equiv e(\phi - \phi_s)/T = (1 - M^2)/2$, describe localized acceleration to supersonic velocities (the subscript s denotes values at the sonic plane, here at the neck of the nozzle). The potential is found from the Boltzmann relation. The DL according to these relations, exhibited in Fig. 2, is similar to that described in Ref. [7]. Note that in the subsonic regime the plasma accelerates along the converging magnetic-field lines, in contrast to the expected deceleration due to the magnetic-mirror effect.

In a diverging-only cross section, acceleration to supersonic velocities can occur when $\nu \neq 0$, where the ionization provides the drag force [15,17]. The first term on the RHS of Eq. (5) is positive along the acceleration, and the ionization, the second term, is large enough in the subsonic regime to make the RHS of the equation negative. We identify the source of a *localized DL acceleration*, observed for this configuration experimentally [6,8] and in simulations [19], as the simultaneous and abrupt cross-section expansion and ionization variation, such as in
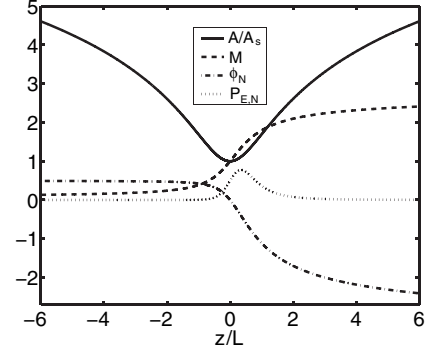

FIG. 2. The DL in a plasma flow along a converging-diverging magnetic field (similar to [7]). Shown are the profiles of the normalized (as defined in the text) cross section A/A_s, Mach number M, potential ϕ_N, and electrostatic pressure $P_{E,N}$.

the forms: $(A/A_s)/\sqrt{1 + 2\ln(A/A_s)} = 1 + \ln[1 + (z/L)^2]$ and $\nu = (c/2)/[1 + \ln(A/A_s)]d\sqrt{1 + 2\ln(A/A_s)}/dz$. With these specified A and ν, we are able to express the flow variables as:

$$A = A_s\exp\left(\frac{M^2 - 1}{2}\right), \qquad n = \frac{n_sA_s}{A}\sqrt{\frac{2}{M^2 + 1}},$$

$$\phi_N = \frac{1 - M^2}{2} + \ln\sqrt{\frac{2}{M^2 + 1}}, \qquad (6)$$

$$1 + \ln\left[1 + \left(\frac{z}{L}\right)^2\right] = \frac{\exp[(M^2 - 1)/2]}{M}.$$

The dependence of M on z in the last expression holds also for the flow shown in Fig. 2.

Figure 3(a) shows the profiles of A/A_s, M, ϕ_N, and $\nu_N \equiv 10\nu L/c$. Figure 3(b) shows the momentum balance along the acceleration region, the contributions of the axial pressure P_b and of the pressure at the radial boundaries P_w, and their sum P_t, which is the accumulating momentum gain, all normalized to the electron pressure upstream, n_0TA_0:

$$P_b \equiv \frac{n_0TA_0 - nTA}{n_0TA_0} = 1 - \frac{1}{\sqrt{M^2 + 1}},$$

$$P_w \equiv \frac{\int_{A_0}^A nTdA'}{n_0TA_0} = \sqrt{M^2 + 1} - 1, \qquad (7)$$

$$P_t \equiv \frac{m\Gamma\nu A}{n_0TA_0} = \frac{M^2}{\sqrt{M^2 + 1}}.$$

These expressions and Fig. 3 show that the main contribution to the momentum gain is P_w, the plasma pressure at the radial boundaries of the diverging flow (where it is balanced by the external force, the magnetic-field force). Also shown in Figs. 2 and 3(b) is the normalized electrostatic pressure $P_{E,N} \equiv (1/2)[d\phi_N/d(z/L)]^2 = [(\epsilon_0/2) \times (d\phi/dz)^2/n_0T]L^2/\lambda_D^2$, where $\lambda_D^2 \equiv \epsilon_0T/(e^2n_0)$. Since $L^2/\lambda_D^2 \gg 1$ (several hundreds in [6]), the contribution of the electrostatic pressure to the momentum is indeed negligible.
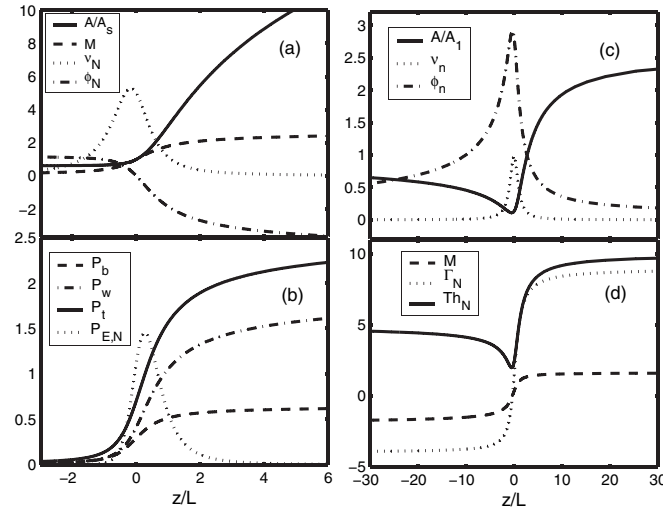
FIG. 3. (a),(b) The DL in a plasma flow along a divergent magnetic field (similar to [6,8]). Shown are (a) the normalized cross section A/A_s, Mach number M, ionization frequency ν_N, and potential ϕ_N, and (b) the normalized axial plasma pressure P_b, pressure at the radial boundaries P_w, their sum P_t, and the electrostatic pressure $P_{E,N}$. (c),(d) Plasma is accelerated in both directions along field lines and there is no potential difference between the two opposite plasma edges. Shown are (c) the normalized cross section A/A_1, ionization frequency ν_n, and potential ϕ_n, and (d) the Mach number M, and the normalized plasma flux Γ_N and thrust Th_N.

The last configuration [Figs. 3(c) and 3(d)] corresponds to a possible (although not optimized) laboratory thruster, as well as to possible acceleration of plasma in space. There is no potential difference between the two opposite plasma edges (no need for a "battery"), the only energy deposited in the plasma is that for ionization and for providing thermal energy. The plasma is generated near the maximum of the magnetic-field intensity (a minimum of the flow cross section) and is accelerated in both directions along field lines. Figure 3(c) shows the spatial profiles of the normalized flow cross section A/A_1, ionization collision frequency $\nu_n \equiv \nu L/c$, and electric potential $\phi_n \equiv e(\phi - \phi_1)/T$ (the subscript 1 denotes values at $z = -\infty$). The force exerted on the plasma by the asymmetrical magnetic field imparts a larger momentum to the right than to the left. As a result, as is shown in Fig. 3(d), although the flow velocity to the left is larger than to the right, the particle flux $\Gamma_N \equiv nAM/n_1A_1$ and the thrust $\text{Th}_N \equiv nA(M^2 + 1)/n_1A_1$ are larger to the right, exhibiting an electrodeless accelerator without end walls. The relations between the flow variables in Figs. 3(c) and 3(d) are: $\nu = (3.0815c/\pi L)/[1 + (z/L)^2]$, $(3.0815/\pi)[\arctan(z/L) + \pi/2] = 2(M + 2) - 4\ln[(M + 4)/2]$, $A/A_1 = [(M + 4)/2]^{17}\exp(1.5M^2 - 4M - 14)$, and $n/n_1 = (M + 4)A_1/2A$.

Abrupt divergence of the magnetic field and localized ionization could result in fast particle beams in space, accelerated by the mechanism described in Fig. 3. Since

the scale length of the acceleration is determined by variations in the magnetic-field topology and by the ionization mean-free-path, solar wind acceleration, for example, could occur, according to a recent intriguing suggestion, in the sun's chromosphere [11], rather than in the corona [16].

In this Letter we have unfolded the sources of the momentum gain in DLs. In a current-carrying 1D DL, in which electromagnetic energy is converted into particle energy, the thrust of the plasma is the same on both sides of the DL, while in a current-free DL along a divergent magnetic field, in which no electromagnetic energy is deposited, the magnetic-field force increases the plasma thrust along the flow. In both DLs the contribution of the electric-field pressure to the momentum is negligible. The quasi-1D model allowed us an analytical description of DL structures in a plasma expanding in a diverging magnetic field. A 2D model should reveal the detailed radial and axial structure of the flow.

[1] M. A. Raadu, Phys. Rep. **178**, 25 (1989).

[2] H. Alfven, Tellus **10**, 104 (1958).

[3] P. Carlqvist, IEEE Trans. Plasma Sci. **14**, 794 (1986).

[4] H. Hora, P. Lalousis, and S. Eliezer, Phys. Rev. Lett. **53**, 1650 (1984).

[5] P. Coakley, N. Hershkowitz, R. Hubbard, and G. Joyce, Phys. Rev. Lett. **40**, 230 (1978).

[6] C. Charles and R. Boswell, Appl. Phys. Lett. **82**, 1356 (2003).

[7] S. A. Cohen et al., Phys. Plasmas **10**, 2593 (2003).

[8] X. Sun et al., Phys. Rev. Lett. **95**, 025004 (2005); O. Sutherland, C. Charles, N. Plihon, and R. W. Boswell, Phys. Rev. Lett. **95**, 205002 (2005).

[9] N. Plihon, C. S. Corr, and P. Chabert, Appl. Phys. Lett. **86**, 091501 (2005).

[10] R. E. Ergun et al., Phys. Plasmas **9**, 3695 (2002); D. L. Newman, M. V. Goldman, R. E. Ergun, and A. Mangeney, Phys. Rev. Lett. **87**, 255001 (2001).

[11] R. W. Boswell, E. Marsch, and C. Charles, Astrophys. J. Lett., "Current-Free Electric Double Layer in a Coronal Magnetic Funnel" (to be published).

[12] D. A. Bryant, R. Bingham, and U. de Angelis, Phys. Rev. Lett. **68**, 37 (1992); J. E. Borovsky, Phys. Rev. Lett. **69**, 1054 (1992).

[13] R. C. Davidson, *Physics of Non-neutral Plasmas* (Imperial College, London, 2001), p. 415.

[14] K. Oswatitsch, *Gas Dynamics* (Academic, New York, 1956), Chap. 2.

[15] A. Fruchtman, N. J. Fisch, and Y. Raitses, Phys. Plasmas **8**, 1048 (2001).

[16] E. N. Parker, *Interplanetary Dynamical Processes* (Interscience, New York, 1963), Chap. V.

[17] W. M. Manheimer and R. F. Fernsler, IEEE Trans. Plasma Sci. **29**, 75 (2001).

[18] M. J. Hole and S. W. Simpson, Phys. Plasmas **4**, 3493 (1997).

[19] A. Meige et al., Phys. Plasmas **12**, 052317 (2005).